Journal of Sol-Gel Science and Technology (2018) 85:743–752
https://doi.org/10.1007/s10971-018-4586-1

ORIGINAL PAPER: SOL-GEL AND HYBRID MATERIALS FOR OPTICAL, PHOTONIC AND OPTOELECTRONIC APPLICATIONS

Preparation of dye-sensitized solar cells using template free TiO_2 nanotube arrays for enhanced power conversion

N. Sriharan[1] · N. Muthukumarasamy[2] · T. S. Senthil[1] · Misook Kang[3]

Received: 22 June 2017 / Accepted: 15 January 2018 / Published online: 5 February 2018

Abstract

By using the vertically aligned ZnO nanorod arrays (NRAs), TiO_2 nanoparticles attached ZnO nanorods (TiO_2@ZnO) and TiO_2 nanotube arrays (NTAs) were prepared from feasible seed-induced template free sol-gel dip coating method. TiO_2 NTAs were prepared by removing the ZnO nanorod cores using wet-chemical etching. By using TiO_2 NTAs as working electrode, dye-sensitized solar cell with enhanced power conversion efficiency was obtained. To verify the formation of TiO_2 NTAs various characterization techniques such as X-ray diffraction, UV-VIS absorbance spectra, Field Emission Scanning Electron Microscopy (FESEM), Energy-Dispersive Spectra (EDS), and High-Resolution Transmission Electron Microscopy (HRTEM) have been used. X-ray diffraction patterns of ZnO NRAs and TiO_2@ZnO NRAs indicate that prepared films possess both the ZnO wurtzite (002) and TiO_2 anatase (101) phase. FESEM image clearly shows that vertically aligned ZnO nanorods having the diameter and length of ~180–240 nm and ~1.5 μm, respectively, have been formed. The FESEM image also clearly showed that diameter and length of TiO_2@ZnO NRAs are ~250–320 nm and ~1.5 μm, respectively. By using UV-VIS absorption spectra, the band gap of vertically aligned ZnO NRAs, TiO_2@ZnO NRAs, and TiO_2 NTAs have been calculated and its values were 3.14, 3.20, and 3.52 eV, respectively. The dye-sensitized solar cell was prepared by using three different working electrodes ZnO NRAs, TiO_2@ZnO, and TiO2 NTAs. The power conversion efficiency of dye-sensitized solar cells prepared using ZnO NRAs, TiO_2@ZnO, and TiO_2 NTAs are 3.53%, 4.04%, and 5.18%, respectively. TiO_2 NTAs with 10 s HCl etching exhibited the highest photoelectric conversion efficiency of 5.18% with short-circuit photocurrent density (J_{sc}) = 13.34 mA/cm^2 and open-circuit photovoltage (V_{oc}) = 0.63 V.

✉ T. S. Senthil
tssenthi@gmail.com

[1] Department of Physics, Erode Sengunthar Engineering College, Erode 638476, India

[2] Department of Physics, Coimbatore Institute of Technology, Coimbatore 641 014, India

[3] Department of Chemistry, Yeungnam University, Gyeongbuk 712-749, South Korea

Graphical Abstract

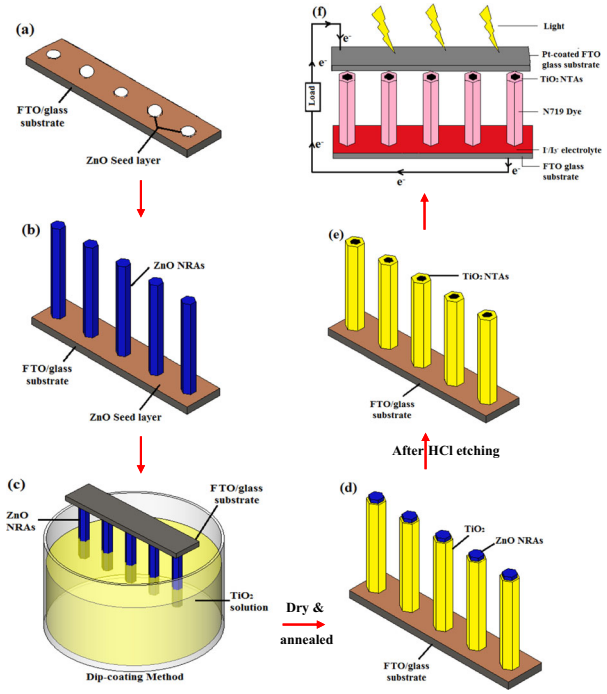

Keywords TiO_2 NTAs · ZnO NRAs · Template free · Dye-sensitized solar cell

Highlights:

- Template free TiO_2 nanotube arrays were prepared from simple sol-gel method
- TiO_2 nanoparticles decorated/attached ZnO nanorods (TiO_2@ZnO) are synthesized
- The maximum power conversion efficiency of 5.18% was obtained for nanotube based solar cell

1 Introduction

Fabrication of high efficiency and low-cost solar cell are the prime issues in the field of photovoltaics. Comparing the factors that affect the efficiency shows the low-surface recombination is one of the prerequisites for the enhancement of efficiency. Manufacturing of efficient photovoltaic power products with low cost in large volumes is the main challenging task. Among the semiconductors available TiO_2 is an important candidate for working electrode in dye-sensitized solar cells [1]. Nanocrystalline TiO_2 is a good solar cell material exhibiting long life time and stability and which when used in solar cell is capable of yielding high efficiency [2]. Recent research is focused on enhancing the power conversion efficiency, having a systematic understanding of material properties and initiating new preparation techniques.

The performance of nanocrystalline TiO_2 thin film based dye-sensitized solar cell is extremely dependent on various parameters among them crystallinity, surface morphology, and crystalline phase are important [3, 4]. Due to this, intense investigation has been initiated to synthesize various nanostructured TiO_2 thin films with size-related electrical and optical properties [5, 6]. TiO_2 nanostructures with various surface morphologies like nanotube [7–10], nanowire [11–16], nanospheroidal [17], cauliflower-like structure [18], nanorod [19, 20], brookite nanoflower like structure [5], nanofiber [21, 22], nanobelt [23], nanocrystals [24], nanoleaves [25], some hierarchical patterns, and so on [26] have been prepared from diverse methods. Although, TiO_2 nanocrystals with different shapes have been prepared by using various methods, the reason for the different structure formation mechanism is still a challenge.

The existing titanium precursors, such as chloride or alkoxide are extremely reactive with water; making shape control of TiO_2 very difficult. Recently, Qui [27, 28] and Na et al. [29] have reported a novel approach to fabricate TiO_2 nanoparticles attached ZnO nanorods (TiO_2@ZnO). Compared with all other nanostructures, tube like structure is the most appropriate structure to attain great enhancement

in the surface area without increasing the geometric area. This structure is also suitable for unidirectional electron transport. A dense network of TiO_2 nanotubes should be favorable for electron collection, because this nanotube structure alone provides more direct conduction path for electrons to travel from the point of injection to the collection electrode. A theoretical study says that nanotubes have high-dye molecule absorbing area compared to nanocrystals [30]. Recently, Adachi et al. [11] reported that the DSSC with TiO_2 nanotube (TiO_2 NT) arrays gave more than twice the photocurrent of DSSC with TiO_2 nanoparticles. TiO_2 nanotube structures have been synthesized by large number of techniques, such as anodic oxidation [31], sol-gel [32], microwave irradiation [33], hydrothermal [34], and template synthesis [35]. Among them, sol-gel method is a comparatively simple technique for the preparation of aligned TiO_2 nanotube arrays.

Grätzel and their research group successfully developed thick spin coated nanoporous TiO_2 films as photoelectrode in DSSCs and have reported high-power conversion efficiency (PCE) of about 10.4% [36]. One of our previous work demonstrated that TiO_2 nanoparticles deposited on ZnO nanorods can be used as a photoanode and resulted in an enhanced PCE of 3.25% [37]. In particular, Kuang et al. [38] studied the importance of TiO_2 nanotubes as working electrode in dye-sensitized solar cell and they achieved a maximum PCE of 3.6%. Recently, Madhavan et al. assembled DSSC consisting of g-C_3N_4/TiO_2, a composite material comprising graphitic carbon nitride and titania as a photoanode with 2-aminopyrimidine incorporated polymer electrolyte and achieved an improved PCE of upto 4.73% [39]. Hence, most of the recent research is focussed on to study the influence of redox electrolyte mixed with potassium iodide (KI), iodine (I_2), and 4-tert-butylpyridine (TBP) on the power conversion enhancement.

Most of the researchers prepared TiO_2 nanotubes by using alumina as template and synthesizing nanotubes without template is challenging one. In this study, we have made an attempt to prepare template free TiO_2 NTAs using ZnO nanorods. The crystallinity, structure, and morphology of ZnO NRAs and TiO_2 NTAs have been studied. Dye-sensitized solar cell was assembled by using TiO_2 NTAs as working electrode and platinum coated counter electrode and their characteristics has been studied.

2 Experimental details

2.1 Preparation of ZnO nanorod arrays

All the chemicals used in this experiment are of high purity purchased from Aldrich and were used without further purification. Milli-Q water has been used for the experiments. Fluorine doped tin oxide (FTO-10 Ω) glass substrates were cleaned in ultrasonic bath with acetone and 2-propanal successively for 30 min and then by drying in nitrogen atmosphere.

ZnO NRAs were grown perpendicular to the FTO substrates. Briefly, ZnO seed layer has been prepared by using sol-gel dip coating method. To prepare ZnO seed layer, 4.0 g of zinc acetate dihydrate ($Zn(CH_3COO)_2.2H_2O$) was dissolved in a mixture of 0.4 ml of 2-methoxyethanol ($CH_3OCH_2CH_2OH$) and 0.3 ml of monoethanolamine ($HOCH_2CH_2NH_2$) at room temperature. The solution was stirred at 60 °C for 30 min to yield a homogeneous solution, finally the FTO glass substrate was dipped in the solution and withdrawn from the solution at a rate of 1.5 cm/min. The prepared seed layers were annealed at 550 °C for 1 h to form ZnO seed layer on the FTO glass substrates. Subsequently, an aqueous precursor solution was prepared by dissolving 0.4 g of zinc nitrate hexahydrate ($Zn(NO_3)_2.6H_2O$) and 0.9 g of hexamine ($(CH_2)_6N_4$) in 30 ml of Milli-Q water. The ZnO seed layer was immersed in the mixed solution at 90 °C for 5 h without magnetic stirring. ZnO seed layer surface was covered by ZnO nanorod arrays. Then the resultant FTO glass substrate was washed by Milli-Q water to remove the remaining salt from the surface of the film and annealed at 550 °C for 1 h in air atmosphere and the schematic diagrams of ZnO seed layer and ZnO nanorods are shown in Fig. 1a, b.

2.2 Preparation of TiO_2 @ ZnO nanorods

In brief, 9 ml of n-tetrabutyltitanate $(Ti(OC_4H_9n)^4$ was mixed in the blend solution of 40 ml ethanol (C_2H_5OH) and 2.5 ml of di-ethanolamine $NH(C_2H_5OH)_2$. The blended solution was stirred at room temperature for 3 h, the obtained solution was hydrolyzed by adding blend of 0.5 ml Milli-Q water and 5 ml of ethanol drop wise under continuous stirring. Again after 3 h continuous stirring, TiO_2 solution was saved in bottle for a period of 48 h. ZnO nanorod coated FTO substrate was dipped inside the prepared TiO_2 solution (Fig. 1c) and the FTO substrate was removed with a withdrawal speed of 3 cm/min. TiO_2 nanoparticles attached ZnO thin films were dried at 90 °C for 15 min, and annealed at 550 °C for 1 h at 3 °C/min in air to obtain TiO_2@ZnO NRAs and it is shown in Fig. 1d.

2.3 Eliminating the ZnO nanorod arrays

TiO_2@ZnO NRAs were dipped in 4% (v/v %) HCl acid solution at room temperature for 5 and 10 s. Finally, the prepared TiO_2 NTAs were washed thoroughly with milliq water to remove the unwanted residual materials and dried in open air atmosphere and it is shown in Fig. 1e.

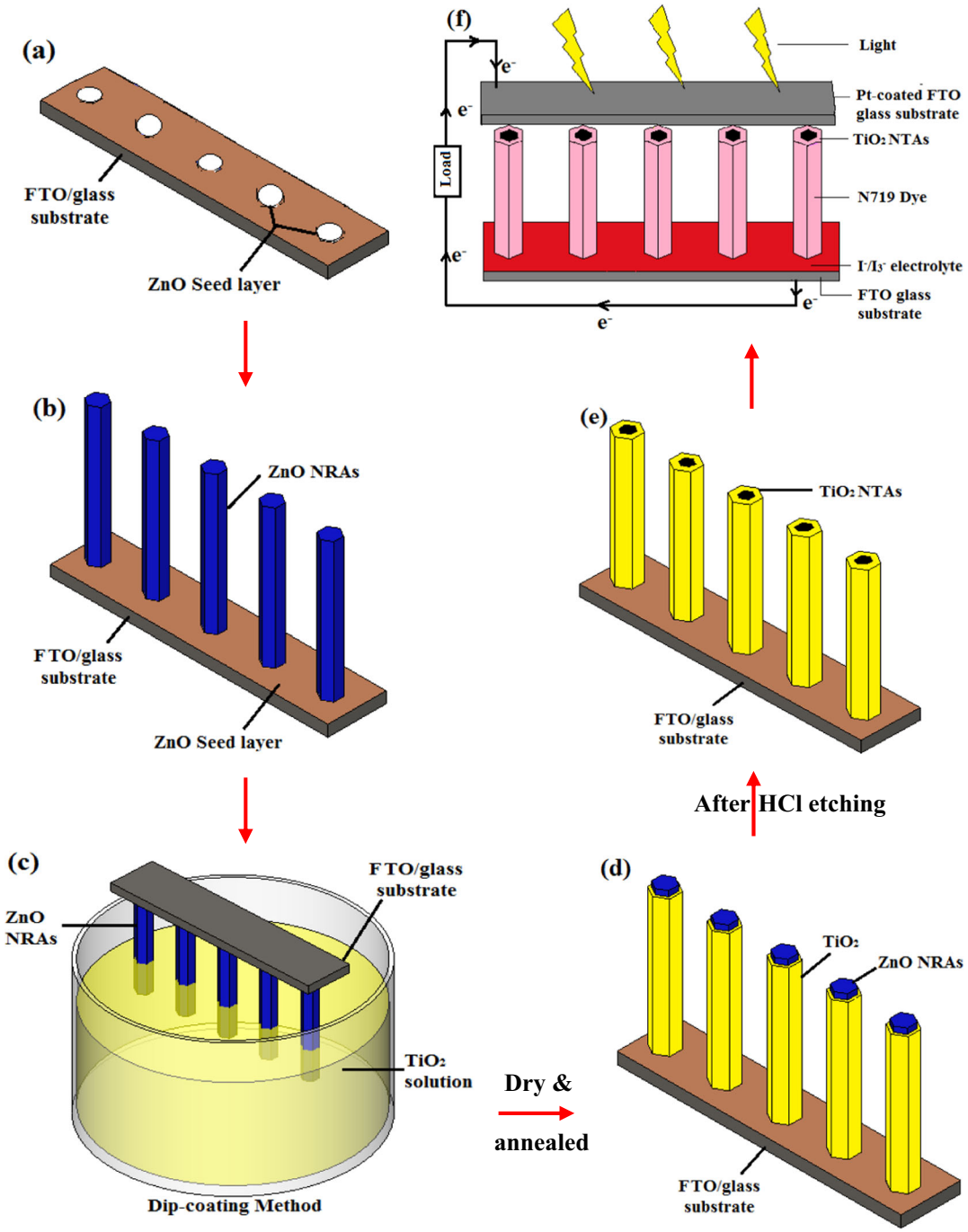

Fig. 1 Schematic illustrations of **a** ZnO seed layer, **b** ZnO NRAs, **c** ZnO NRAs immersed in TiO_2 solution, **d** TiO_2@ZnO NRAs, **e** TiO_2 NTAs after wet-chemical etching, and **f** fabricated device using TiO_2 NTAs

2.4 Assembling the dye-sensitized solar cells

To prepare dye-sensitized solar cells, the prepared working electrodes, such as ZnO NRAs, TiO_2@ZnO NRAs, and TiO_2 NTAs (Fig. 1f) were immersed in 0.3 mM N719 dye solution for 24 h. After that period, the dye-sensitized electrodes were rinsed with ethanol and dehydrated. The dye adsorbed working electrode was placed over the commercially available platinum coated FTO electrode, and the cell edges were sealed by using a sealing sheet (PECHM-1, Mitsui- Dupont Polychemical) with hot plate at 110 °C for 3 min. To make a contact between working electrode and counter electrode a redox electrolyte was used and it was prepared by mixing 0.5 mol KI with 0.05 mol I_2 and 0.5 mol

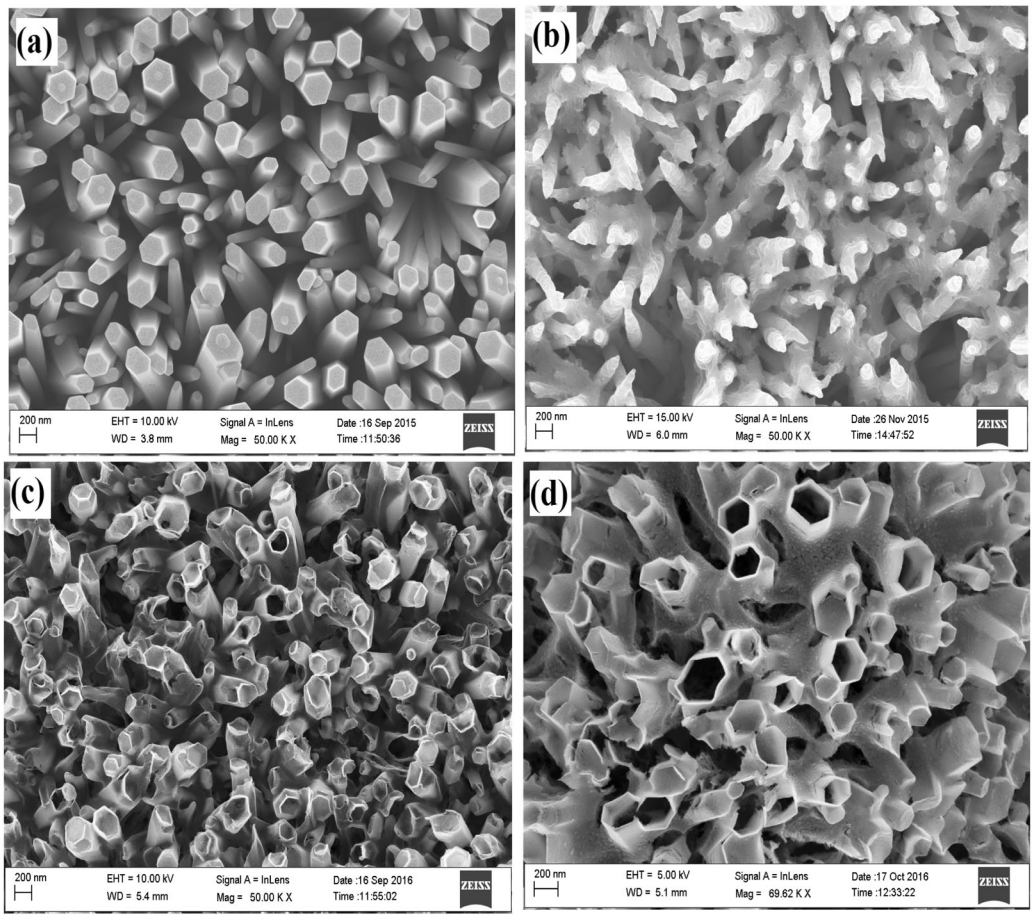

Fig. 2 Top-view FESEM images of **a** vertically aligned ZnO NRAs, **b** ZnO NRAs coated with TiO_2, TiO_2 NTAs after wet-chemical etching at **c** 5 s and **d** 10 s

4-tert-butylpyridine. A drop of liquid electrolyte was injected into the platinum coated counter electrode and was driven into the cell. Finally, the holes of the counter electrode were sealed by using scotch tapes and the size of the working electrode was 0.4 (0.5 x 0.8) cm^2.

2.5 Characterization

The surface morphology of prepared thin films was observed using a field emission scanning electron microscope (FESEM: S-4700, ZEISS). X-ray diffraction (XRD) analysis was performed by using Bruker AXS (D8 ADVANCE) X-ray diffractometer under Cu Kα (30 kV, 30 mA) radiation. Transmission electron microscopy (TEM: JEM200CX, JEOL) with an energy-dispersive X-ray analyzer (EDX: OXFORD) was used to observe the crystal structure of the TiO_2 NTAs. UV-VIS double beam absorbance spectra of the prepared films were recorded using a Hitachi Corporation UV-2700 spectrophotometer. The photocurrent–voltage (I–V) curves were recorded using white light from a xenon lamp (max. 150 W) using a sun 2000 solar simulator (ABET Technologies). Light intensity was adjusted by using Si solar cell to ~AM-1.5. Incident light intensity and active cell area were 100 mW/cm^2 (one sun illumination) and 0.4 cm^2, respectively.

3 Results and discussion

3.1 FESEM analysis

Figure 2 depicts the FESEM images of ZnO NRAs, TiO_2@ZnO NRAs, and TiO_2 NTAs. Figure 2a exhibits the surface top view of vertically aligned ZnO nanorods, the diameter and length of the ZnO NRAs are ~180–240 nm and ~1.5 µm, respectively. Figure 2b shows the FESEM image of ZnO NRAs coated with TiO_2 nanoparticles. The diameter and length of ZnO NRAs coated with TiO_2 nanoparticles are ~250–320 nm and ~1.5 µm, respectively. These results indicate that the TiO_2 nanoparticles are attached on the outer surface of the ZnO NRAs. In order to optimize the wet-chemical etching time, the grown ZnO

NRAs were etched with 3% (v/v%) diluted HCl. Initially, TiO_2 NTAs are etched using diluted HCL solution for ~ 5 s and the corresponding SEM image is shown in Fig. 2c. The image clearly shows that there is a partially top-opened ZnO NRAs and it cannot be totally removed. It shows that 5 s etching cannot produce hollow TiO_2 NTAs. So the etching time is increased to 10 s and its SEM image is shown in Fig. 2d. The image shows that there is subsequently stable TiO_2 NTAs grown on the substrate. TiO_2 NTAs are of ~1.5 µm length and ~260–410 nm in inner diameter with open-ended hexagonal tube-like structure covering the entire surface of the FTO substrate.

3.2 XRD analysis

Figure 3 portrays the XRD patterns for vertically aligned ZnO NRAs, TiO_2@ZnO NRAs, and TiO_2 NTAs. The peaks present at 31.8°, 34.5°, 36.3°, 47.6°, 56.6, 62.9°, and 68.0° corresponds to (100), (002), (101), (102), (110), (103), and (112) planes of ZnO wurtzite structure (JCPDS no. 36-1451) [40]. The strongest peak at $2\theta = 34.5°$ corresponds to (002) plane and it is observed in both the XRD patterns of ZnO NRAs and TiO_2@ZnO NRAs. It clearly indicates that the preferential crystal growth along the *c*-axis direction is due to the typical crystal habit and growth form of ZnO wurtzite structure [41, 42]. ZnO NRAs coated with TiO_2 exhibit a pattern, which is shown in Fig. 3b and it reveals that there is a small peak at $2\theta = 25.4°$ which corresponds to (101) plane of polycrystalline TiO_2 anatase phase (JCPDS no. 21-1272) [43, 44]. These results indicate that ZnO NRAs coated with TiO_2, possess both the ZnO wurtzite (002) and TiO_2 anatase (101) phase. Figure 3c shows the diffraction pattern of TiO_2 NTAs on the FTO substrate. Here, TiO_2 anatase stands in form of NTAs due to is higher acid resistance. After wet-chemical etching, no characteristic peaks corresponding to ZnO NRAs is observed in the pattern. The peaks detected on the as-synthesized TiO_2 NTAs can be indexed to anatase TiO_2.

3.3 UV-visible analysis

UV-vis absorption spectra of vertically aligned ZnO NRAs, ZnO NRAs coated with TiO_2 and TiO_2 NTAs are shown in Fig. 4. The absorption edges are around 394.5, 386.9, and 351.3 nm for ZnO NRAs, ZnO NRAs coated with TiO_2 and TiO_2 NTAs, respectively. This reveals that all the samples exhibit sharp absorption in the UV region. The absorption edge is shifted toward lower wavelength region when ZnO NRAs surface morphology is modified into TiO_2 NTAs. The values of band gap were calculated by extrapolation of absorption edge on to the *x*-axis. The observed band gap of the vertically aligned ZnO NRAs, ZnO NRAs coated with TiO_2 and TiO_2 NTAs have been calculated and its values were 3.14 eV, 3.20, and 3.52 eV, respectively.

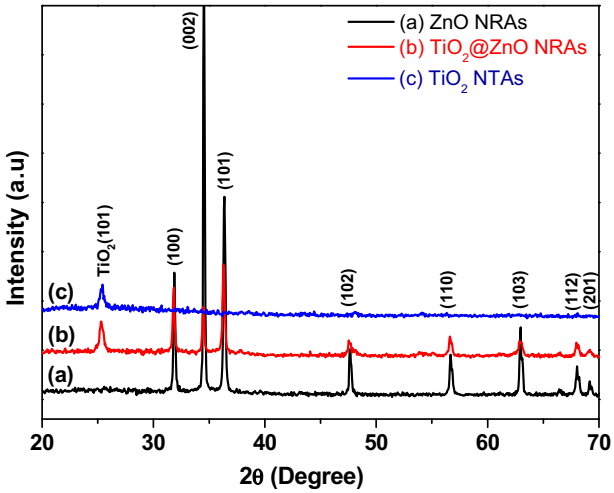

Fig. 3 XRD Patterns of **a** vertically aligned ZnO NRAs, **b** ZnO NRAs coated with TiO_2, and **c** TiO_2 NTAs after wet-chemical etching

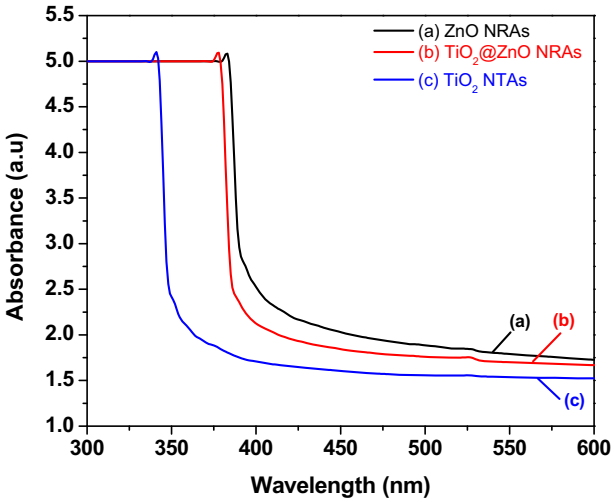

Fig. 4 UV-Visible absorption spectra of **a** vertically aligned ZnO NRAs, **b** ZnO NRAs coated with TiO_2, and **c** TiO_2 NTAs after wet-chemical etching

3.4 HRTEM analysis

Figure 5 depicts the HRTEM and SAED images of the typical TiO_2 nanotube. From Fig. 5a, we can find that after wet-chemical etching, TiO_2 NT with open-end and hexagonal tube-like structure with diameter of ~300 nm has been formed with identical wall thickness of ~20 nm, respectively. Figure 5b is the HRTEM image taken from the part of single nanotube consisting of small crystallites with a size of 4–5 nm. The observed average *d*-spacing values 0.354 and 0.238 nm agree well with the standard *d*-spacing

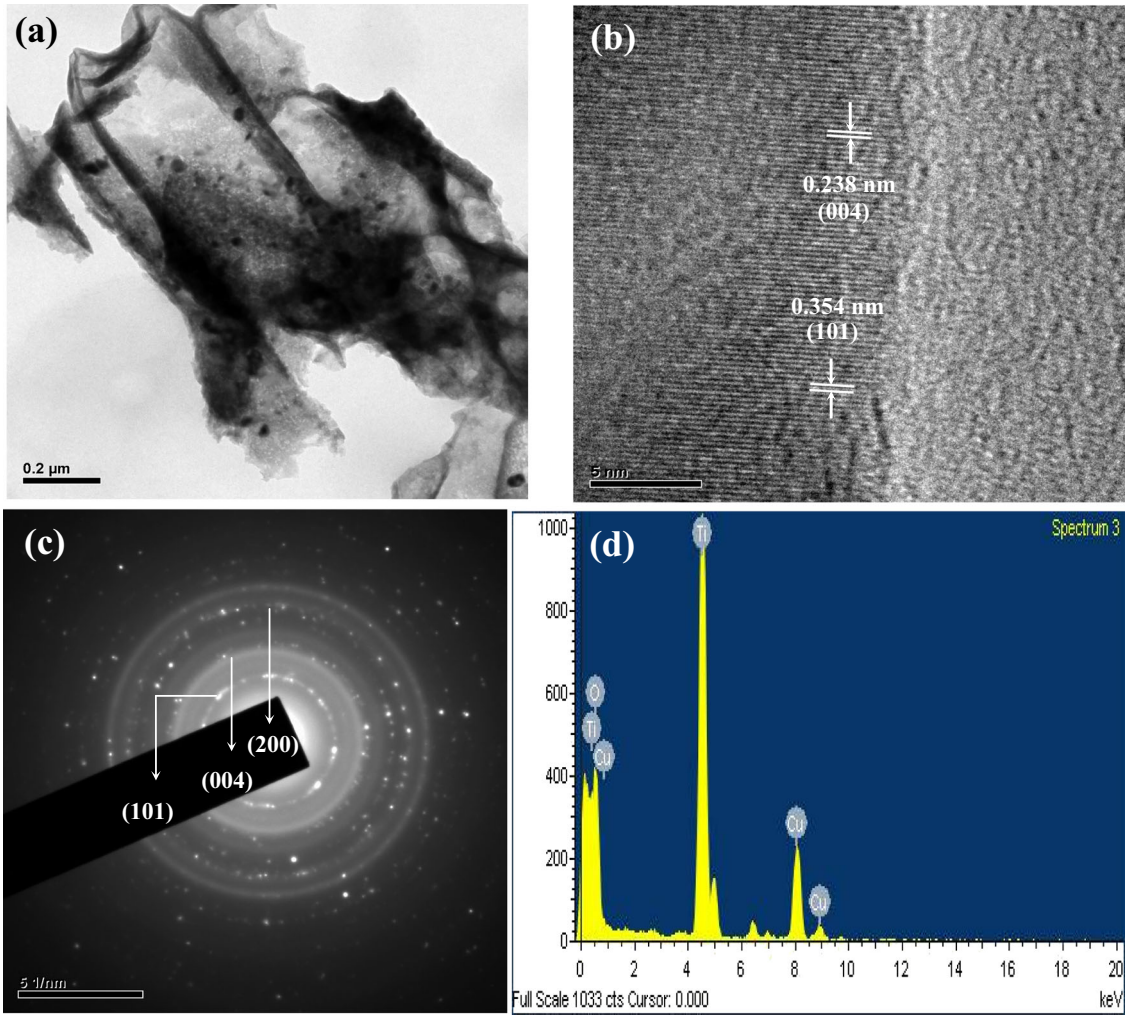

Fig. 5 **a**, **b** HRTEM image, **c** SAED Pattern, and **d** EDS spectrum of the synthesized TiO_2 NTAs after 10 s HCl etching

values and it corresponds to (101) and (004) planes of anatase phase (JCPDS no. 21-1272) [45, 46], confirming that the nanotube is TiO_2. This result is in good agreement with the XRD pattern shown in Fig. 2c. Figure 5c shows the SAED pattern of TiO_2 nanotube and it exhibits diffraction rings. Bright diffraction rings correspond to (101), (004), and (200) planes of TiO_2, and it indicates that TiO_2 nanotubes of anatase phase is formed. Energy dispersive spectrum analysis (EDS) was carried out to identify the elemental composition of TiO_2 nanotube and it is shown in Fig. 5d. The figure clearly shows that TiO_2 nanotube is composed of O and Ti only and the remaining peaks are due to the Cu grids which are used for TEM analysis.

3.5 *J-V* Characteristics

The photocurrent density−photovoltage (*J-V*) characteristics of the prepared dye-sensitized solar cell are shown in Fig. 6a, b. The dye-sensitized solar cells prepared using ZnO nanorod as photoanode shows the short-circuit photocurrent density $(J_{sc}) = 9.35\ mA/cm^2$, open-circuit photovoltage $(V_{oc}) = 0.58\ V$ and power conversion efficiency = 3.53%. TiO_2 nanoparticles attached ZnO nanorods shows the power conversion efficiency of 4.04% with $J_{sc} = 10.69\ mA/cm^2$ and $V_{oc} = 0.629\ V$. However, for TiO_2 NTA based DSSCs, the J_{sc}-values obviously increased to $13.34\ mA/cm^2$.

A maximum power conversion efficiency of 5.18% is achieved for the TiO_2 NTAs with 10 s HCl etching. This may be attributed to the formation of open-ended hexagonal hollow tube-like structures on the working electrode and this has resulted in more dye molecule adsorption. Whereas the working electrode prepared using 5 s HCl etched TiO_2 NTAs shows only 4.7%, which may due to the partially top-opened ZnO nanorods. Compared with partially top-opened ZnO nanorods, open-ended hexagonal hollow tube-like structures provide large specific surface area, which absorb more dye molecules and produces more photo-electrons.

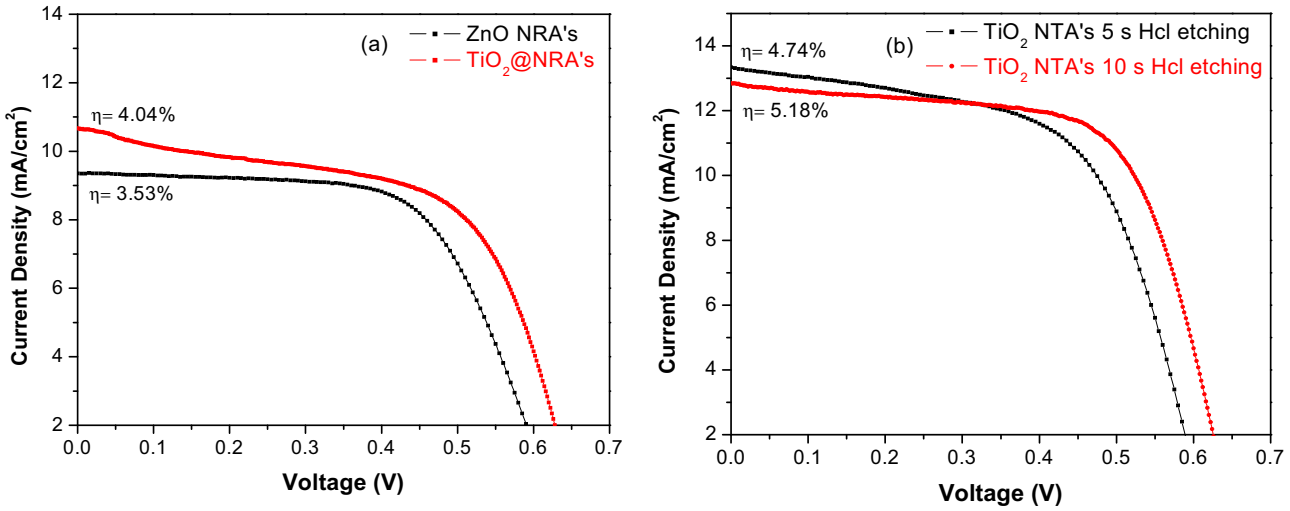

Fig. 6 *J-V* Characteristics of DSSC prepared using **a** ZnO NRAs and TiO_2@ZnO NRAs **b** TiO_2 NTAs

Even though TiO_2 NTAs with 5 s HCl etching shows higher J_{sc} (13.34 mA/cm^2) than the TiO_2 NTAs with 5 s HCl etching (12.86 mA/cm^2), the reduced power conversion efficiency may be due to the variation in V_{oc}. The V_{oc} reduction in TiO_2 NTAs with 5 s HCl etching may be due to the faster charge recombination at the partially top opened TiO_2@ZnO/electrolyte interface [47].

The obtained efficiencies are better than the efficiency of TiO_2 NTA based DSSCs prepared by Na et al. and Kim et al. [29, 48] and is the best power conversion efficiency reported so far for TiO_2 NTA based dye-sensitized solar cells in which the TiO_2 NTA were grown using a template free method. Kim et al. have prepared conical islands shaped TiO_2 NTAs and have reported a maximum power conversion efficiency of 1.8%. Na et al. have reported about the preparation of vertically aligned TiO_2 nanotubes using electrochemically deposited ZnO nanorods. They have reported that the maximum power conversion efficiency for TiO_2 nanotube based dye-sensitized solar cell is only 0.20%.

4 Conclusion

By using simple sol-gel dip coating template free method TiO_2 NTAs have been prepared using vertically aligned ZnO nanorods. The TiO_2 nanotube arrays are successfully prepared by removing the ZnO nanorod cores using wet-chemical etching and the effect of chemical etching has also been analysed. X-ray diffraction patterns of ZnO NRAs and TiO_2@ZnO NRAs indicates that the prepared films possess both the ZnO wurtzite (002) and TiO_2 anatase (101) phase. FESEM image clearly shows that vertically aligned ZnO nanorods having the diameter and length of ~180–240 nm and ~1.5 µm, respectively. The FESEM image also clearly showed that diameter and length of TiO_2@ZnO NRAs are ~250–320 nm and ~1.5 µm, respectively. By using the prepared ZnO NRAs, TiO_2@ZnO NRAs and TiO_2 NTAs as working electrode dye-sensitized solar cells have been fabricated. The power conversion efficiency of dye-sensitized solar cells prepared using ZnO NRAs, TiO_2@ZnO, and TiO_2 NTAs are 3.53, 4.04, and 5.18%, respectively. The maximum power conversion efficiency of 5.18% with short-circuit photocurrent density (J_{sc}) = 13.34 mA/cm^2 and open-circuit photovoltage (V_{oc}) = 0.63 V was obtained for the dye-sensitized solar cells prepared using the TiO_2 NTAs working electrode etched using HCl for 10 s.

Acknowledgements This work was supported and grants funded by the Science and Engineering Research Board (SERB), a Statutory Body under Department of Science and Technology (DST), New Delhi (SR/FTP/PS-114/2012), for which the authors are very grateful.

Compliance with ethical standards

Conflict of interest The authors declare that they have no competing interest.

References

1. Ghande AR, Fernandez JO (2005) A simple method to synthesize light active N-Doped anatase (TiO_2) photocatalyst. Bull Catal Soc India 4:131–134
2. Alex S, Santhosh U, Das S (2005) Dye sensitization of nano-crystalline TiO_2: enhanced efficiency of unsymmetrical versus symmetrical squaraine dyes. J Photochem Photobiol A Chem 172:63–71
3. Ding Z, Lu GQ, Greenfield PF (2000) Role of the crystallite phase of TiO_2 in heterogeneous photocatalysis for phenol oxidation in water. J Phys Chem B 104:4815–4820

4. Seo J, Chung H, Kim M, Lee J, Choi I, Cheon J (2007) Small, development of water-soluble single-crystalline TiO_2 nanoparticles for photocatalytic cancer-cell treatment. Small 3:850–853
5. Zhao B, Chen F, Huang Q, Zhang J (2009) Brookite TiO_2 nanoflowers. Chem Commun 34:5115–5117
6. Wang F, Shi Z, Gong F, Jiu J, Adachi M (2007) Morphology control of anatase TiO_2 by surfactant-assisted hydrothermal method. Chin J Chem Eng 15(5):754–759
7. Chen S, Paulose M, Ruan C, Mor GK, Varghese OK, Kouzoudis D, Grimes CA (2006) Electrochemically synthesized CdS nanoparticle-modified TiO_2nanotube-array photoelectrodes: preparation, characterization, and application to photoelectrochemical cells. J Photochem Photobiol A Chem 177:177–184
8. Varghese OK, Paulose M, Shankar K, Mor GK, Grimes CA (2005) Water-photolysis properties of micron-length highly-ordered titania nanotube-arrays. J Nanosci Nanotech 5: 1158–1165
9. Li X, Cheng Y, Liu L, Mu J (2010) Enhanced photoelectrochemical properties of TiO_2 nanotubes co-sensitized with CdS nanoparticles and tetra sulfonated copper phthalocyanine. Colloids Surf A Physicochem Eng Asp 353:226–231
10. Mor GK, Shankar K, Paulose M, Varghese OK, Grimes CA (2006) Use of highly-ordered TiO_2 nanotube arrays in dye-sensitized solar cells. Nano Lett 6:215–218
11. Adachi M, Murata Y, Takao J, Jiu J, Sakamoto M, Wang F (2004) Highly efficient dye-sensitized solar cells with a titania thin-film electrode composed of a network structure of single-crystal-like TiO_2 nanowires made by the "oriented attachment" mechanism. J Am Chem Soc 126:14943–14949
12. Wei M, Zhi-mei Q, Ichihara M, Honma I, Zhou H (2006) Ultra-long single-crystal TiO_2-B nanowires: synthesis and electrochemical measurements. Che Phys Lett 424:316–320
13. Lin Y, Wu GS, Yuan XY, Xie T, Zhang LD (2003) Fabrication and optical properties of TiO_2 nanowire arrays made by sol–gel electrophoresis deposition into anodic alumina membranes. J Phys 15:2917
14. Miao Z, Xu DS, Ouyang JH, Guo GL, Zhao XS, Tang YQ (2002) Electrochemically induced sol−gel preparation of single-crystalline TiO_2 nanowires. Nano Lett 2:717–720
15. Lee JH, Leu IC, Hsu MC, Chung YW, Hon MH (2005) Fabrication of aligned TiO_2 one-dimensional nanostructured arrays using a one-step templating solution approach. J Phys Chem B 109(27):13056–13059
16. Wu JM, Shih HC, Wu WT, Tseng YK, Chen IC (2005) Thermal evaporation growth and the luminescence property of TiO_2 nanowires. J Cryst Growth 281:384–390
17. Sudhagar P, Jung JH, Park S, Sathyamoorthy R, Ahn H, Kang YS (2009) Self-assembled CdS quantum dots-sensitized TiO_2 nano-spheroidal solar cells: structural and charge transport analysis. Electrochem Acta 55:113–117
18. Yang L, Lin Y, Jia J, Xiao X, Li X, Xiaowen Z (2008) Light harvesting enhancement for dye-sensitized solar cells by novel anode containing cauliflower-like TiO_2 spheres. J Power Sour 182 (1):370–376
19. Jiu J, Isoda S, Wang F, Adachi M (2006) Dye-sensitized solar cells based on a single-crystalline TiO_2 nanorod film. J Phys Chem B 110(5):2087–2092
20. Yoshida R, Suzuki Y, Yoshikawa S (2005) Syntheses of TiO_2(B) nanowires and TiO_2 anatase nanowires by hydrothermal and post-heat treatments. J Solid State Chem 178:2179–2185
21. Li D, Xia Y (2003) Fabrication of titania nanofibers by electrospinning. Nano Lett 3(4):555–560
22. Ostermann R, Li D, Yin Y, McCann JT, Xia Y (2006) V_2O_5 nanorods on TiO_2 nanofibers: a new class of hierarchical nanostructures enabled by electrospinning and calcination. Nano Lett 6 (6):1297–1302
23. Pan K, Dong Y, Tian C, Zhou W, Tian G, Zhao B, Fu H (2009) TiO_2-B narrow nanobelt/TiO_2 nanoparticle composite photoelectrode for dye-sensitized solar cells. Electrochem Acta 54 (28):7350–7356
24. Balraju P, Kumar M, Roy MS, Sharma GD (2009) Dye sensitized solar cells (DSSCs) based on modified iron phthalocyanine nanostructured TiO2 electrode and PEDOT:PSS counter electrode. Synth Met 159(13):1325–1331
25. Wen P, Itoh H, Feng Q (2006) Preparation of nanoleaf-like single crystals of anatase-type TiO_2 by exfoliation and hydrothermal reactions. Chem Lett 35:1226–1227
26. Zhang Y, Zhang J, Wang P, Yang G, Sun Q, Zheng J, Zhu Y (2010) Anatase TiO_2 hollow spheres embedded TiO_2 nanocrystalline photoanode for dye-sensitized solar cells. Mater Chem Phys 123:595–600
27. Qui JJ, Jin Z, Liu Z, Liu X, Liu G, Wu W, Zhang X, Gao X (2007) Fabrication of TiO_2 nanotube film by well-aligned ZnO nanorod array film and sol-gel process. Thin Solid Films 515:2897–2902
28. Qui JJ, Yu W, Gao X, Li X (2006) Sol-gel assisted ZnO nanorod array template to synthesize TiO_2 nanotube arrays. Nanotechnology 17:4695–4698
29. Na S-I, Kim S-S, Hong W-K, Park J-W, Jo J, Nah Y-C, Lee T, Kim D-Y (2008) Fabrication of TiO_2 nanotubes by using electrodeposited ZnO nanorod template and their application to hybrid solar cells. Electrochim Acta 53:2560–2566
30. Jiang CY, Sun XW, Lo GQ, Kwong DL (2007) Improved dye-sensitized solar cells with a ZnO-nanoflower photoanode. Appl Phys Lett 90:263501
31. Mor GK, Varghese OK, Paulose M, Grimes CA (2005) Transparent highly ordered TiO_2 nanotube arrays via anodization of titanium thin films. Adv Funct Mater 15:1291–1296
32. Yang S, Liu Y, Sun C (2006) Preparation of anatase TiO_2/Ti nanotube-like electrodes and their high photoelectrocatalytic activity for the degradation of PCP in aqueous solution. Appl Catal A 301(2):284–291
33. Wu X, Jiang QZ, Ma ZF, Fu M, Shangguan WF (2005) Synthesis of titania nanotubes by microwave irradiation. Solid State Commun 136:513–517
34. Ou H, Lo S (2007) Review of nanotubes synthesized via hydrothermal treatment: fabrication, modification and application. Sep Purif Technol 58:179–191
35. Na SI, Kim SS, Hong WK, Park J, Jo J, Nah YC, Lee T, Kim DY (2008) Fabrication of TiO_2 nanotubes by using electrodeposited ZnO nanorod template and their applicationto hybrid solar cells. Electrochem Acta 53(5):2560–2566
36. Nazeeruddin MK, Kay A, Rodicio I, Humpbry-Baker R, Miiller E, Liska P, Vlachopoulos N, Gratzel M (1993) Conversion of light to electricity by cis-XzBis(2,2'-bipyridyl-4,4'-dicarboxylate)ruthenium(11) charge-transfer sensitizers (X = $C1^-$, Br^-, I^-, CN^-, and SCN^-) on nanocrystalline TiO_2 electrodes. J Am Chem Soc 115 (14):6382–6390
37. Senthil TS, Muthukumarasamy N, Kang Misook (2013) Applications of highly ordered paddle wheel like structured ZnO nanorods in dye sensitized solar cells. Mater Lett 102–103:26–29
38. Kuang D, Brillet J, Chen P, Takata M, Uchida S, Miura H, Sumioka K, Zakeeruddin SM, Gratzel M (2008) Application of highly ordered TiO_2 nanotube arrays in flexible dye-sensitized solar cells. ACS Nano 2(6):1113–1116
39. Senthil RA, Theerthagiri J, Madhavan J, Murugan K, Arunachalam P, Arof AK (2016) Enhanced performance of dye-sensitized solar cells based on organic dopant incorporated PVDFHFP/PEO polymer blend electrolyte with g-C_3N_4/TiO_2 photoanode. J Solid State Chem 242(1):199–206
40. Huang YM, Ma QL, Zhai BG (2013) A simple method to grow one-dimensional ZnO nanostructures in air. Mater Lett 93:266–268

41. Vayssieres L (2003) Growth of arrayed nanorods and nanowires of ZnO from aqueous solutions. Adv Mater 15(5):464–466
42. Laudise RA, Kolb ED, Caporason AJJ (1964) Hydrothermal growth of large sound crystals of zinc oxide. J Am Ceram Soc 47:9–12
43. Chen Y, Huang W, He D, Situ Y, Huang H (2014) Construction of heterostructured g-C_3N_4/Ag/TiO_2 microspheres with enhanced photocatalysis performance under visible-light irradiation. ACS Appl Mater Interfaces 6(16):14405–14414
44. Zhou X, Peng F, Wang H, Yu H, Fang Y (2012) A simple preparation of nitrogen doped titanium dioxide nanocrystals with exposed (001) facets with high visible light activity. Chem Commun 48(4):600–602
45. Varghese OK, Paulose M, Shankar K, Mor GK, Grimes CA (2005) Water-photolysis properties of micron-length highly-ordered titania nanotube arrays. J Nanosci Nanotechnol 5: 1158–1165
46. Paulose M, Mor GK, Varghese OK, Shankar K, Grimes CA (2006) Visible light photoelectrochemical and water-photoelectrolysis properties of titania nanotube arrays. J Photochem Photobiol A 178:8–15
47. Li H, Yu Q, Huang Y, Yu C, Li R, Wang J, Guo F, Zhang Y, Zhang X, Wang P, Zhao L (2016) Ultra-long rutile TiO_2 nanowire arrays for highly efficient dye-sensitized solar cells. ACS Appl Mater Interfaces 8(21):13384–13391
48. Kim W-R, Park H, Choi W-Y (2015) Conical islands of TiO_2 nanotube arrays in the photoelectrode of dye-sensitized solar cells. Nanoscale Res Lett 10:63